Electronic structure and contact resistance at an open-end carbon nanotube and copper interface

Feng Gao,[1] Jianmin Qu,[1,a)] and Matthew Yao[2]
[1]*Department of Civil and Environmental Engineering, Northwestern University, Evanston, Illinois 60208, USA*
[2]*Rockwell Collins Inc., Cedar Rapids, Iowa 52498, USA*

(Received 8 January 2010; accepted 10 February 2010; published online 11 March 2010)

We report a quantum mechanics study on the electronic structure and contact resistance at an open-end carbon nanotube and copper interface. The local density of states near the carbon nanotube (CNT)/Cu interface are computed using density functional theory (DFT), and the transmission coefficient is calculated using a nonequilibrium Green's function method in conjunction with DFT. The current-voltage relation of the simulating cell is obtained by using the Landauer–Buttiker formula, from which the contact resistance can be determined. Our results indicate that the contact resistance of the Cu/CNT/Cu system is comparable to that of solder/Cu interface in electronic packaging. © *2010 American Institute of Physics*. [doi:10.1063/1.3354077]

Carbon nanotubes (CNTs) have emerged as one of the most promising candidates for nanoscale electronic devices owing to their size, structural strength, and excellent thermal and electronic properties.[1,2] For potential electronic applications, one of the key issues is often the contact between CNT and the metallic electrodes.[3] An individual semiconducting CNT can operate either as a conventional metal-oxide semiconductor field-effect transistor or an unconventional Schottky barrier transistor when it makes a contact with a metal electrode. Thus the interaction and the resulting electronic structure between CNTs and metal electrode are crucial for the performance of a potential device.

Several studies have been conducted to investigate the electronic characteristics between CNTs and various metal electrodes, such as Ti, Pd, Cu, Au, Mo, Ni, Pt, etc.[3–8] These studies mainly focus on the side-contact between CNTs and metal electrodes. In many applications, end-contact is more prevalent.[9–11] In this letter, we report a study on the end-contact between SWCNT and Cu electrodes using first principles calculations. For comparison purposes, the side-contact case is also considered. Copper was selected as the electrode because of its extensive use in integrated circuits.[12,13] Most relevant to this study are the recent works by Andriotis and Menon,[14,15] where the embedded-contact and side-contact between CNT and Ni electrode have been reported.

Our calculations were conducted on a two-probe model comprised of a semiconducting (10, 0) SWCNT with each end in contact with a Cu electrode either in an end-contact or a side-contact configuration, as shown in Figs. 1(a) and 1(b). The CNT is approximately 1 and 1.5 nm long for the end-contact and side-contact configuration, respectively. Each Cu electrode consisted of $5\times5\times4$ atoms. The separation distance between the CNT and Cu is ~1.85 Å for end-contact and 1.20 Å for side-contact. These distances were determined by minimizing the interaction energy of the system to ensure a stable configuration. The separation distance for side-contact is measured between the nearest pair of Cu and C atoms. The simulations were performed using the ATK TOOLKIT code[16] based on the density functional theory (DFT) with double-ξ plus polarization basis sets.

To calculate the electronic structure and transport properties, the DFT simulation is combined with the Keldysh nonequilibrium Green's function (NEGF) method. The interaction of the left- and right-electrodes on the scattering region is taken into account through self-energies. In order to calculate the contact resistance of the CNT/Cu interface, a bias voltage is prescribed across the two-probe system by setting the left electrode at zero voltage and the right electrode at $V>0$. A steady-state current is then generated and flows along the CNT axis. The bias voltage provides natural electrostatic boundary conditions for the Hartree potential in the scattering region, which is self-consistently solved on a three-dimensional (3D) real space grid. The electron transport direction along the tube axis is the z-direction, and the other two orthogonal directions are the x- and y-directions. All calculations were performed based on the generalized gradient approximation with Perdew–Burke–Ernzerhof pseudoatomic potentials. The k-point sampling in the Brillouin zone integration parameters is 3, 3, and 50 in x-, y-, and z-directions, respectively. The energetic convergence criterion for the Hamiltonian, charge density, and band-structure energy is 1×10^{-5}.

To understand the interaction between the C and Cu atoms at an end-contact, the local density of states (LDOS) at the Fermi level ($E_F=0$) was calculated in the k-space. Figure 2(a) illustrates the LDOS contour projected onto a particular cross-section plane which is parallel to the CNT axis. At the end-contact Cu/CNT interfaces, the LDOS is significantly

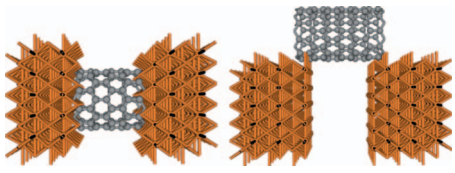

(a) (b)

FIG. 1. (Color) The Cu/CNT/Cu simulation cell used in the study: (a) end-contact and (b) side-contact.

a)Electronic mail: j-qu@northwestern.edu.

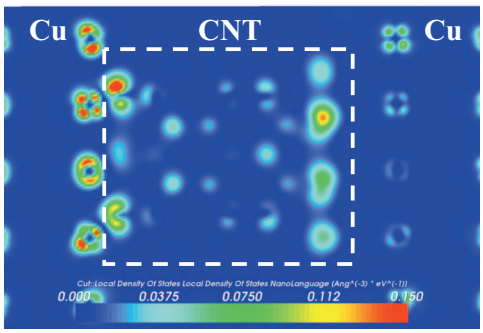

(a)

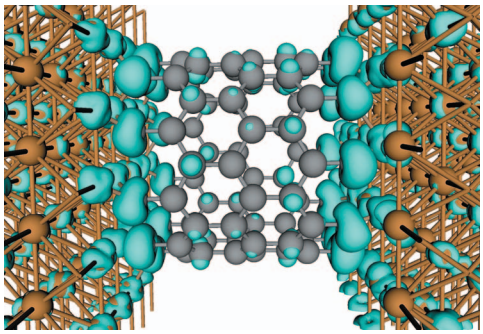

(b)

FIG. 2. (Color) LDOS of end-contact Cu/CNT/Cu two-probe system: (a) 2D LDOS contours. (b) Isosurface plot of LDOS.

enhanced when the Cu and C atoms are relatively close. At the left-interface the LDOS of Cu atoms exhibits quite different contours due to the interaction with C atoms in CNT. The 3D isosurface illustration of LDOS shown in Fig. 2(b) further indicates the C-Cu interaction at the interfaces. These figures clearly show the strong electronic interaction between the CNT and Cu atoms when they form the end-contact, which reflects the potential for electron transport at the contact area.

To characterize the bond between the CNT and Cu electrode, the Mulliken population of the two-probe system was computed to separate the electron density into atomic contributions. The Mulliken overlap population (MOP) between the atoms for a particular orbital was extracted to reveal the bonding characteristics. Figure 3 shows the calculated MOP of the end-contact Cu/CNT/Cu system. Thicker lines represent higher bond strength. Clearly, bond between the C and

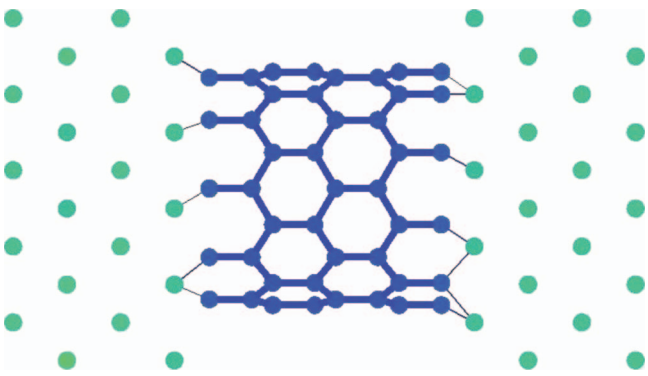

FIG. 3. (Color) MOP of the end-contact Cu/CNT/Cu system: the green dots represent the Cu atoms while the blue dots represent the C atoms.

Cu atoms is formed at the interfaces. This C–Cu bond is much weaker than the C–C bond in CNT as indicated by the line thickness. Our calculated results show that the average bond strength between the C and Cu atom is only about 1/4 that of the C–C bond in CNT. Note that the metallic bond between the Cu atoms is not illustrated here.

To compute the Cu/CNT interfacial contact resistance, the I-V relationship of the two-probe system is needed. This can be obtained by using the Landauer–Buttiker formula, which relates the conductance to the transmission probability $T(E,V)$,[17]

$$I(V) = \frac{2e}{h}\int_{\mu_1}^{\mu_2} dET(E,V)[f(E-\mu_1) - f(E-\mu_2)], \qquad (1)$$

where μ_1 and μ_2 are the chemical potential of left and right electrodes, $f(E-\mu)=1/\{1+\exp[E-\mu/k_BT_{\text{temp}}]\}$ is the Fermi–Dirac distribution function, k_B is the Boltzmann constant, and T_{temp} is the temperature, and $T(E,V)$ is the transmission function. The transmission function can be computed through the independent $\mathbf{k}_{\|}$ (surface-parallel direction reciprocal lattice vector point) channels and their integral over the two-dimensional (2D) reciprocal unit cell $\tilde{\Omega}$,

$$T(E,V) = \frac{1}{\Omega}\int_{\tilde{\Omega}} d\mathbf{k}_{\|} T^{\mathbf{k}_{\|}}(E,V), \qquad (2)$$

where Ω is the area of the reference unit cell surface. In computing $T^{\mathbf{k}_{\|}}$, the matrix version of NEGF approach was

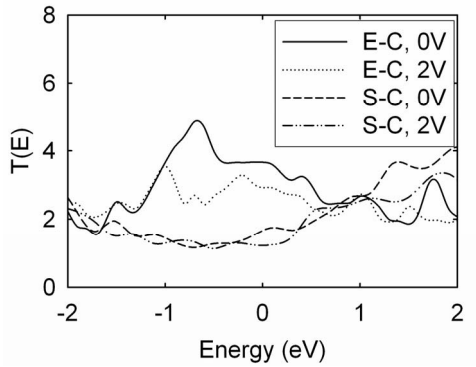

(a)

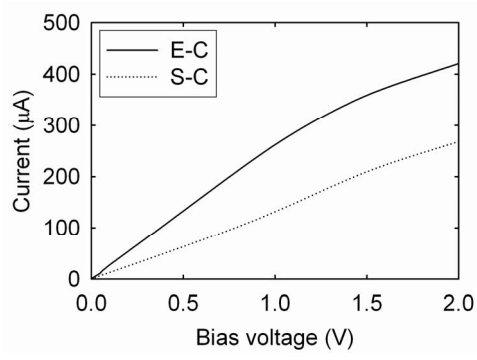

(b)

FIG. 4. (a) Transmission coefficient vs energy level at various bias voltages for both the end-contact and side-contact configurations and (b) corresponding I-V curves of both types of CNT/Cu contacts. The "E-C" represents "end-contact," while "S-C" represents "side-contact."

used. The NEGF is a well-developed general formalism to treat various nonequilibrium charge transport phenomena.[18]

The calculated transmission spectrums under different bias voltage are shown in Fig. 4(a). The zero energy reference is taken at the Fermi level E_F. It is seen that, at the lower bias voltages <0.1 V, the transmission coefficient spectrum is almost invariant to the bias voltage over the range of energy level shown here. However, at higher bias voltages (>1.0 V), the amplitude of transmission coefficient is much lower around the Fermi level ($E_F=0$). This indicates that the electron transport is much stronger at lower bias than at higher bias. Moreover, the side-contact configuration exhibits a lower electron transmission performance, particularly around the Fermi energy.

Making use of the transmission function shown in Fig. 4(a) in conjunction with Eq. (1), the *I-V* relationships can be obtained. Presented in Fig. 4(b) is the corresponding *I-V* curves for both end-contact and side-contact configurations. Once the *I-V* relationship is known, the total resistance of the system can be computed via the Ohmic law, if the *I-V* curve is linear. This is the case for low bias. By averaging the data below 0.1 V, we calculated the total resistance of the Cu/CNT/Cu system as 3.64 kΩ for end-contact and 7.84 kΩ for side-contact.

To find out whether the resistance of the two-probe system calculated above is dependent on the length of the CNT tube, we have conducted another set of computations where the CNT length is doubled. The results show that doubling the CNT length does not change the total resistance of the two-probe system. One may thus conclude that much of the resistance is attributed to the contact resistance at the CNT/Cu interfaces.

To place above values in perspective, we note that Andriotis and Menon have reported similar values for CNT in end-contact with Ni.[14] Although it is not directly comparable, Goddard and co-workers[7] have reported much higher contact resistance values for graphene in contact with Cu electrode.[2] Furthermore, for both types of CNT/Cu contacts, the resistance computed here is comparable to the that at the solder/Cu interface used commonly in microelectronic packaging nowadays. This is an indication that CNT has the potential to replace solder as the electrical interconnect in electronic packaging.

In summary, our simulation results show that the electronic structure at the CNT/Cu interface is significantly altered by C and Cu interaction. The Cu–C bond strength is only about 1/4 that of the C–C bond in CNT. The CNT/Cu end contact resistivity is ~ 1.50 kΩ nm^2. This result shows the feasibility of using open-end CNT to replace solder alloys as electrical interconnects in microelectronic packaging.

The authors acknowledge the financial support from Rockwell Collins Inc, Contract No. 1806F51.

[1] S. Iijima, Nature (London) **354**, 56 (1991).
[2] T. Rueckes, K. Kim, E. Joselevich, G. Y. Tseng, C. L. Cheung, and C. M. Lieber, Science **289**, 94 (2000).
[3] W. G. Zhu and E. Kaxiras, Nano Lett. **6**, 1415 (2006).
[4] S. Dag, O. Gulseren, S. Ciraci, and T. Yildirim, Appl. Phys. Lett. **83**, 3180 (2003).
[5] N. Park and S. Hong, Phys. Rev. B **72**, 045408 (2005).
[6] T. Z. Meng, C.-Y. Wang, and S.-Y. Wang, J. Appl. Phys. **102**, 013709 (2007).
[7] Y. Matsuda, W.-Q. Deng, and W. A. Goddard, J. Phys. Chem. C **111**, 11113 (2007).
[8] Y. Matsuda, W.-Q. Deng, and W. A. Goddard, J. Phys. Chem. C **112**, 11042 (2008).
[9] J. J. Palacios, A. J. Perez-Jimenez, E. Louis, E. SanFabian, and J. A. Verges, Phys. Rev. Lett. **90**, 106801 (2003).
[10] J. Taylor, H. Guo, and J. Wang, Phys. Rev. B **63**, 245407 (2001).
[11] P. Pomorski, C. Roland, and H. Guo, Phys. Rev. B **70**, 115408 (2004).
[12] T. J. Licata, E. G. Colgan, and J. M. E. Harper, IBM J. Res. Dev. **39**, 419 (1995).
[13] V. V. Talanov, A. Scherz, and A. R. Schwartz, Appl. Phys. Lett. **88**, 262901 (2006).
[14] A. N. Andriotis and M. Menon, Phys. Rev. B **76**, 045412 (2007).
[15] A. N. Andriotis and M. Menon, Phys. Rev. B **78**, 235415 (2008).
[16] ATK/VNL, 2008.10 version, www.quantumwise.com.
[17] S. Datta, *Quantum Transport: Atom to Transistor* (Cambridge University Press, Cambridge, UK, 2005).
[18] Y.-H. Kim, J. Tahir-Kheli, P. A. Schultz, and W. A. Goddard III, Phys. Rev. B **73**, 235419 (2006).